JOC The Journal of Organic Chemistry

Article

pubs.acs.org/joc

Fmoc-Based Synthesis of Disulfide-Rich Cyclic Peptides

Olivier Cheneval,[†,§] Christina I. Schroeder,[†,§] Thomas Durek,[†] Phillip Walsh,[†] Yen-Hua Huang,[†] Spiros Liras,[‡] David A. Price,[‡] and David J. Craik*[,†]

[†]Institute for Molecular Bioscience, The University of Queensland, Brisbane, 4072, QLD Australia

[‡]Worldwide Medicinal Chemistry, CVMED, Pfizer, 610 Main Street, Cambridge, Massachusetts 02139, United States

Supporting Information

ABSTRACT: Disulfide-rich cyclic peptides have exciting potential as leads or frameworks in drug discovery; however, their use is faced with some synthetic challenges, mainly associated with construction of the circular backbone and formation of the correct disulfides. Here we describe a simple and efficient Fmoc solid-phase peptide synthesis (SPPS)-based method for synthesizing disulfide-rich cyclic peptides. This approach involves SPPS on 2-chlorotrityl resin, cyclization of the partially protected peptide in solution, cleavage of the side-chain protecting groups, and oxidization of cysteines to yield the desired product. We illustrate this method with the synthesis of peptides from three different classes of cyclic cystine knot motif-containing cyclotides: Möbius (M), trypsin inhibitor (T), and bracelet (B). We show that the method is broadly applicable to peptide engineering, illustrated by the synthesis of two mutants and three grafted analogues of kalata B1. The method reduces the use of highly caustic and toxic reagents and is better suited for high-throughput synthesis than previously reported methods for producing disulfide-rich cyclic peptides, thus offering great potential to facilitate pharmaceutical optimization of these scaffolds.

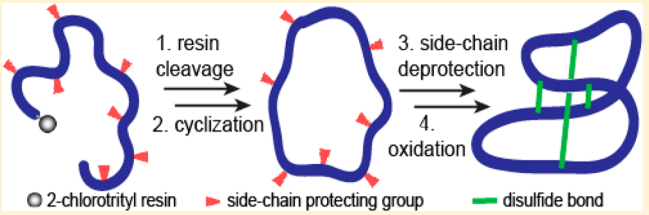

INTRODUCTION

Disulfide-rich cyclic peptides occur in a wide variety of plants and animals, with cyclotides[1−3] being the largest family of these peptides reported to date. Cyclotides are macrocycles of 28−37 amino acids and contain three disulfide bonds arranged in a cyclic cystine knot (CCK) motif.[1] This compact structure confers exceptional stability, with cyclotides being resistant to thermal, chemical, or enzymatic challenges.[4] As a result, cyclotides are emerging as promising drug design scaffolds for the incorporation of pharmaceutically active epitopes.[5−8] Of particular importance from a drug delivery perspective, a recent study by Wong et al. showed oral analgesic activity for the cyclotide kalata B1 grafted with a bradykinin B1 receptor antagonist sequence.[9]

Interest within the drug discovery community toward disulfide-rich peptides has increased mainly due to two landmark events: the approval of ziconotide (SNX-111; Prialt), a calcium channel blocker, in the US in 2005 for the treatment of chronic pain (intrathecal injection), and more recently by the approval of linaclotide, an agonist of guanylate cyclase 2C (oral delivery). Both peptides bind to challenging drug targets that demonstrate the therapeutic potential of this modality. The oral administration of linaclotide in particular establishes the importance of the stability of disulfide-rich peptides toward the acidic nature of the stomach and proteases expressed in the gut. The incorporation of a head-to-tail cyclic backbone into disulfide-rich peptide frameworks offers great potential for the further enhancement of stability, making cyclic disulfide-rich peptides such as those having a CCK framework interesting targets for a number of applications.

To enable the successful advancement of compounds through clinical trials, it is imperative to develop robust methodologies to afford high yielding and scalable synthetic procedures that deliver material with high purity and consistent impurity profiles. Synthesis of peptides containing a cyclic backbone is typically achieved by solid-phase peptide synthesis (SPPS) of an acyclic (linear) precursor followed by an on-resin or in-solution intramolecular reaction linking C- and N-termini.[10] In early studies, the cyclization of disulfide-containing peptides[11−13] was traditionally achieved through an adaptation of the elegant native chemical ligation (NCL) method developed by Kent and co-workers.[14] NCL relies on the mutual reactivity of an N-terminal cysteine and a C-terminal thioester and, thus, permits a wide variety of synthetic strategies for cysteine-rich molecules. The construction of the required thioester intermediates is more problematic but can be achieved directly by insertion of a thioester moiety and Boc-SPPS[15] or, indirectly, through the use of various thioester surrogates and Fmoc chemistry.[16] The former approach demands repeated use of corrosive TFA and of highly toxic hydrogen fluoride (HF) in the final cleavage step, is difficult to parallelize for automated high-throughput synthesis, and can be problematic for a number of acid-sensitive functionalities. These drawbacks can be overcome by milder Fmoc-SPPS;[17] however, current strategies for obtaining the required peptidyl-thioesters often require specialized, noncommercially available reagents, and

Received: March 25, 2014
Published: May 23, 2014

additional reaction steps. Again this can add difficulties to the development process for drug entities.

Here we describe a straightforward methodology for the synthesis of complex disulfide-rich cyclic peptides that avoids these drawbacks and has potential to facilitate the use of disulfide-rich cyclic peptides as drug scaffolds. Peptides are assembled on 2-chlorotrityl chloride (2-CTC) resin, allowing for release under mild conditions (using 1% TFA) and leaving all of the side-chain-protecting groups intact. The linear, side-chain-protected peptides are then head-to-tail cyclized in solution via standard amide bond formation. Side chains can then be fully or partially deprotected using orthogonal strategies to allow for random or selective disulfide bond formation to yield the desired cyclic oxidized product (Scheme 1).

Scheme 1. Fmoc-Based Cyclization of Disulfide-Rich Peptides: (a) Chain Elongation, (b) Linear Side-Chain-Protected Precursor, (c) Cyclic Side-Chain-Protected Peptide, (d) Reduced Fully Deprotected Cyclic Peptide, and (e) Oxidized Final Product*

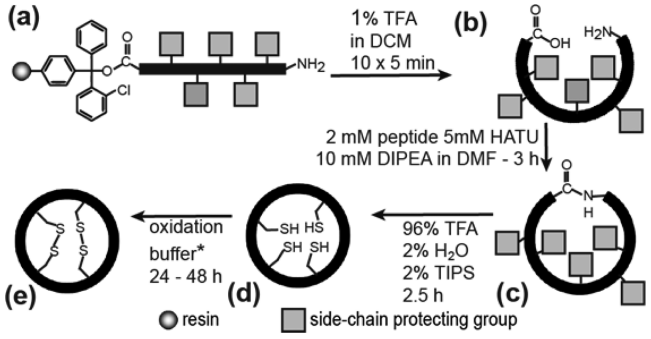

*For oxidation conditions, see Experimental Section.

This strategy has a number of advantages over previous methods, including compatibility with automated Fmoc SPPS, widely available reagents, simple and well understood reaction conditions, and the avoidance of excessive use of hazardous reagents. We applied the approach to the cyclization of peptides from each of the three cyclotide subclasses: kalata B1[18] and its [all-D] enantiomer as the prototypic member of the Möbius class (M), parigidin-br-1 as a representative of the bracelet class (B)[19] and *Momordica cochinchinensis* trypsin inhibitor II (MCoTI-II) as a member of the trypsin inhibitor class (T).[20,21] To further demonstrate the versatility of the method, we also applied it to single-point mutations and grafted analogues of kalata B1 (Figure 1).

RESULTS

The approach outlined in Scheme 1 was applied to the three subfamilies of naturally occurring CCK-containing peptides (Figure 1). To investigate the versatility of the method, we additionally synthesized two kalata B1 peptides containing one point mutation each, [G6A]kalata B1 and [T20S]kalata B1. Previous studies have shown that some of the loops in cyclotides can be replaced (grafted) with a variety of bioactive epitopes to produce hybrid peptides with improved biological activity and stability.[8] We explored whether our new approach was amenable to produce grafted peptides by including an integrin-binding epitope (RGDS) in three of the six loops of kalata B1 (designated as [L2-RGDS]kalata B1, [L3-RGDS]-kalata B1, and [L6-RGDS]kalata B1). In total, nine cyclic peptides ranging in size from 26 to 34 amino acids were synthesized.

Because stepwise SPPS of the linear precursors can, in principle, be started at any residue, we chose different sites of cyclization to explore their effects on chain assembly and cyclization as shown in Figure 1. The chosen cyclization sites are located in loop 2 (Gly/Gly) and loop 6 (Arg(Pbf)/Asn(Trt), Gly/Gly, Asn(Trt)/Gly, Val/Cys(Trt), and Gly/Ser(tBu)) and feature amino acid side chains with varying degrees of steric bulk to investigate the flexibility of the method. Peptide assembly via Fmoc SPPS, cleavage, and cyclization of the native, point mutated, and grafted peptides proceeded smoothly as judged by RP-HPLC and ESI-MS (Supporting Information Figure S2) irrespective of the chosen cyclization points. Oxidative folding of the analogues was carried out under optimized conditions previously established for each class of molecule (see Experimental Section). Characterization data are given in Table 1, and analytical data for each molecule are reported in Supporting Information (Figure S1).

Kalata B1 and its all-D-enantiomer synthesized via the strategy presented in Scheme 1 were obtained in an overall yield of 4.5%, based on resin loading (Figure 2).

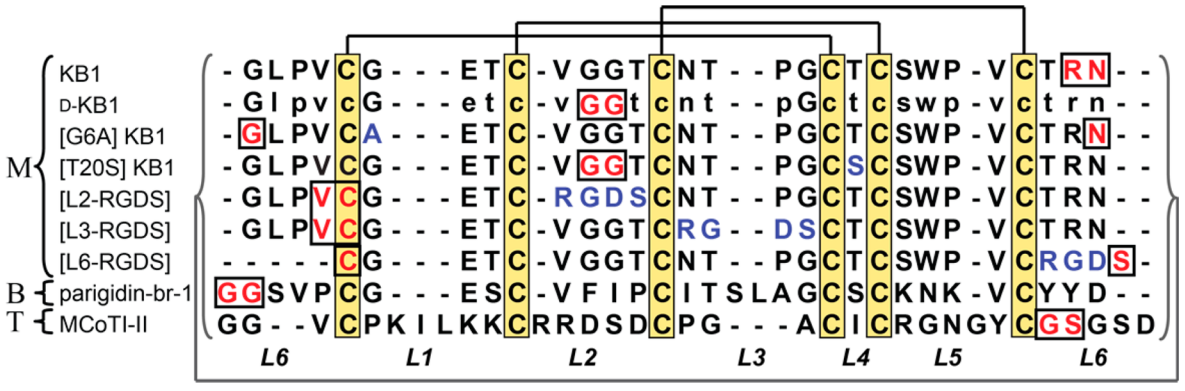

Figure 1. Peptide sequences synthesized in this study. L1–L6 denote the six backbone loops between the conserved Cys residues (highlighted in yellow and connectivity shown at top). Red boxed letters indicate the cyclization site, and letters in blue denote kalata B1 (KB1) mutations. [L2-RGDS], [L3-RGDS], and [L6-RGDS] are grafted KB1 peptides. Lower case letters designate D-amino acids. Cyclotide subfamily: M - Möbius, B - bracelet or T - trypsin inhibitor.

dx.doi.org/10.1021/jo500699m | J. Org. Chem. 2014, 79, 5538–5544

Table 1. Masses, Yields, Retention Times, and Purity of Cyclic, Oxidized Peptides

peptide	calcd mass (Da)[a]	obsd mass (Da)[b]	isolated yield[c] %	isolated yield[c] mg	RT (min)[d]	purity (%)[e]
kalata B1	2892.4	2892.4 ± 0.1	4.5	31.2	27.4	98.5
D-kalata B1	2892.4	2892.5 ± 0.1	4.1	28.1	27.5	99.8
[G6A]kalata B1	2906.4	2906.5 ± 0.1	3.4	23.0	28.1	98.4
[T20S]kalata B1	2878.3	2878.5 ± 0.1	3.8	25.6	27.8	99.2
[L2-RGDS]kalata B1	2993.4	2993.5 ± 0.1	2.8	19.2	23.3	96.9
[L3-RGDS]kalata B1	2938.4	2938.5 ± 0.1	2.1	14.1	25.5	98.2
[L6-RGDS]kalata B1	2569.9	2570.3 ± 0.2[g]	N/A[h]	N/A	N/A	N/A
Parigidin-br-1	3280.8	3280.9 ± 0.1[g]	N/A	N/A	N/A	N/A
MCoTI-II	3453.0	3453.2 ± 0.2	1.8	13.4	13.6	97.2
kalata B1 (Boc)	2892.4	2892.3 ± 0.1	8.1[f]	14.5[f]	27.3	99.6
MCoTI-II (Boc)	3453.0	3452.9 ± 0.2	8.0[f]	16.8[f]	13.4	96.9

[a]Based on weighted average isotope composition. [b]Observed by ESI-MS. [c]Final product yields based on initial resin loading, 0.25 mmol scale synthesis. [d]Observed by LC-MS equipped with a C18, 150 × 2 mm, 5 μm column. Gradient from 2% to 82% of solvent B in solvent A over 40 min. Solvent A: 0.05% formic acid in H_2O; Solvent B: 0.045% formic acid, 10% H_2O, 90% acetonitrile (ACN), temperature 23 °C. [e]As determined by HPLC; based on peak area recorded at 214 nm. [f]Synthesized at 0.0625 mmol scale via manual Boc-SPPS and native chemical ligation. [g]Cyclized effectively, but folding and oxidation did not produce the native/desired connectivity as judged by 2D NMR spectroscopy. [h]N/A: not applicable.

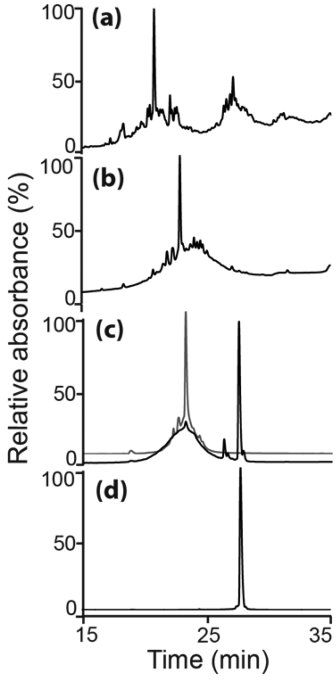

Figure 2. Synthesis of kalata B1 evaluated by HPLC at different stages of the synthesis. (a) Test cleavage of linear kalata B1 after chain assembly by SPPS. (b) Crude cyclic product after cyclization and side-chain deprotection. (c) Crude folding and disulfide formation mixture (black trace) and partially purified, reduced cyclic peptide (gray trace). (d) Purified kalata B1. Analysis was performed using a linear gradient of 2–82% solvent B over 40 min. Absorbance was monitored at 214 nm.

Secondary Hα NMR chemical shifts derived from 2D TOCSY and NOESY NMR spectra of synthetic kalata B1 made via the Fmoc approach were compared to those of kalata B1 obtained via the well-established Boc-SPPS/NCL cyclization approach[11] as well as to those of native peptide isolated from *Oldenlandia affinis*[22] (Figure 3a). Secondary Hα NMR chemical shift measurement is a method used to evaluate differences of backbone Hα chemical shift of amino acids compared to random coil values.[23] This is a sensitive and useful method of identifying changes in the local chemical environment of individual residues.[24] This method is particularly powerful for monitoring folding of peptides during structure–activity studies, and it provides an indication of secondary structure with residues involved in α-helices and β-sheets having negative and positive secondary Hα NMR chemical shift, respectively.

The secondary Hα NMR chemical shifts of all four molecules, kalata B1 (Fmoc), kalata B1 (Boc), isolated kalata B1, and D-kalata B1, were indistinguishable from one another, demonstrating that the correct product had been obtained. Similar results were obtained for the point mutants of kalata B1 ([G6A]/[T20S]) as shown in Figure 3b. In the case of [G6A] kalata B1, a minor but expected difference ($\Delta\delta$ = +0.25 ppm) in the secondary Hα chemical shift was detected for the mutated residue, demonstrating the sensitivity of NMR to detect subtle sequence changes. Furthermore, the cyclic trypsin inhibitor MCoTI-II, the largest macrocyclic peptide examined in this study, was isolated in good yield and was found to be identical to material isolated from *Momordica cochininensis*, as demonstrated by NMR (Figure 4).

The RGDS-grafted kalata B1 peptides were cyclized with similarly high efficiency, but folding and disulfide formation experiments in all cases yielded two major isomers that were separated by RP-HPLC. For [L2-RGDS]kalata B1 and [L3-RGDS]kalata B1, both isomers displayed well dispersed amide protons in 1D ^{1}H NMR spectra indicative of well-ordered tertiary structures. Secondary Hα chemical shifts were used to identify the correct isomers of [L2-RGDS]kalata B1 and [L3-RGDS]kalata B1 by comparing the patterns to wild-type kalata B1 (Figure 3b). Apart from relatively minor differences, which are locally restricted to the modified loops, secondary Hα shifts were in good agreement with native kalata B1. Despite successful assembly and cyclization of [L6-RGDS]kalata B1, neither of the isomers observed in RP-HPLC displayed wide dispersion across the amide proton region, suggesting that in this case the correct disulfide connectivity was not produced.

The bracelet cyclotide parigidin-br-1, like [L6-RGDS]kalata B1, assembled well and yielded the desired cyclized and fully reduced product. However, despite several attempts using a range of different folding conditions, no correctly oxidized product could be obtained as judged by LC-MS and 1D NMR. Möbius and bracelet cyclotide subfamilies are distinguished by

dx.doi.org/10.1021/jo500699m | J. Org. Chem. 2014, 79, 5538–5544

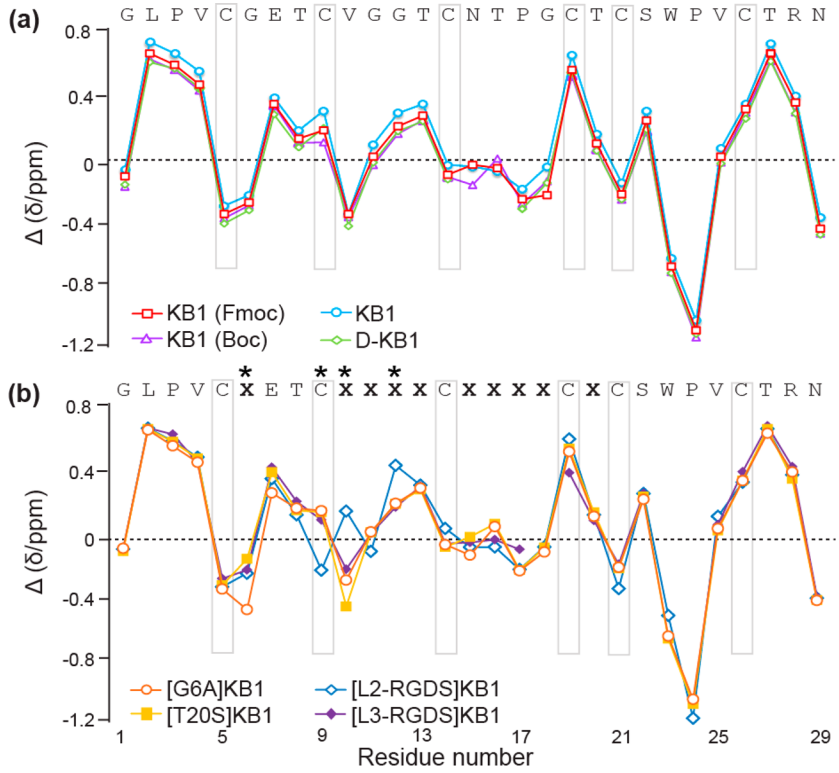

Figure 3. Secondary Hα chemical shifts of kalata B1 and analogues. Sequence for native KB1 is shown at the top, and residue number is shown at the bottom of the graph. X denotes residues that have been replaced in the analogues, and the asterisks indicate residues undergoing chemical shift changes due to the mutations. (a) Secondary Hα chemical shifts of kalata B1 (KB1) isolated from *Oldenlandia affinis* (PDB ID: 1NB1),[22] kalata B1 obtained by Boc chemistry (KB1 (Boc)), kalata B1 (KB1 (Fmoc)) and D-kalata B1 (D-KB1), synthesized using the described method. (b) Secondary Hα chemical shifts of [G6A]KB1, [T20S]KB1, [L2-RGDS]KB1, and [L3-RGDS]KB1.

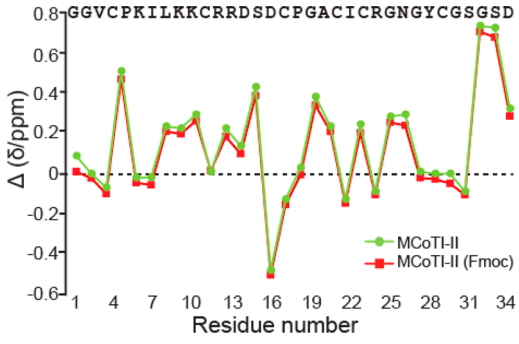

Figure 4. Secondary Hα NMR chemical shifts of native MCoTI-II isolated from *Momordica cochinchinensis* (PDB ID: 1HA9)[21,25] and MCoTI-II synthesized using the Fmoc method described in this work.

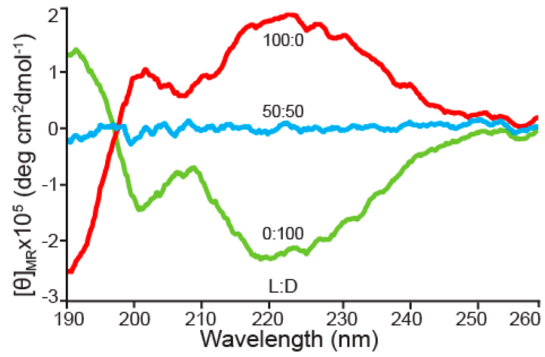

Figure 5. CD spectra of kalata B1 (green) and its all-D enantiomer (red) in aqueous solution (25 μM in H_2O). The CD spectrum of a racemic mixture of both enantiomers is shown in blue.

the presence or absence of a *cis*-proline residue in loop 5, respectively. The presence of the *cis*-proline is believed to force loop 5 into a turn conformation that can function as an efficient nucleation point for peptide folding. Consistent with the findings here, literature studies have reported that bracelet cyclotides are notoriously more difficult to fold than Möbius cyclotides.[26,27]

The enantiomeric relationship of the kalata B1 L- and D-enantiomers was confirmed by CD spectroscopy as described previously.[28] The CD spectra of kalata B1 and its all-D enantiomer reveal equal but opposite mean residue ellipticity ($[\theta]_{MR}$), producing the mirror image relationship between the two peptides seen in Figure 5. The relationship is further highlighted by mixing the L- and the D-enantiomers in a 1:1 ratio, resulting in a CD spectrum with a signal close to zero.

DISCUSSION

Despite more than 100 years of peptide chemistry research and 50 years since the development of SPPS by Merrifield,[29] complex disulfide-rich cyclic peptides remain challenging synthetic targets. The construction of these multimacrocyclic molecules requires additional strategies to overcome the inherent linear design of SPPS, and the 3D structure-stabilizing disulfide cross-links add another level of complexity to synthetic designs. In the past, the combination of Boc-SPPS and NCL has been successful in addressing some of these challenges. Although some problems associated with Boc-SPPS (see above) have been recently overcome through the development of various Fmoc-compatible synthetic procedures[30−35] to

dx.doi.org/10.1021/jo500699m | J. Org. Chem. 2014, 79, 5538−5544

generate the thioester precursors required for NCL, some of these procedures require expert knowledge and specialized reagents that might limit their broader application.

Here we have adapted a straightforward in-solution cyclization approach to chemically access complex disulfide-rich cyclic peptides ranging in size from 26 to 34 amino acids (Scheme S1, Supporting Information). The approach relies on use of the mild-acid cleavable 2-chlorotrityl linker to generate partially protected peptides, which are then head-to-tail cyclized in solution using well established protocols. This approach does not require an N-terminal cysteine residue in the linear precursor and should accommodate a wide variety of synthetic designs. Although racemization (epimerization) of the C-terminal residue during the cyclization step is a possibility, the use of latest generation uronium-type coupling reagents (HATU)[36,37] and sterically hindered bases (*N*,*N*-diisopropylethylamine (DIPEA)) should minimize this potential side reaction. Using high-resolution LC-MS as well as 1D and 2D NMR spectroscopy, we were unable to detect any appreciable racemization in any of the cyclic peptides synthesized, despite considerable variability in the location and sequence environment of the ligation sites (e.g., R/N, N/G, G/G, V/C, S/C, or G/S) (Figure 1). However, due to the complexity of the synthesized 30 amino acid polypeptides, we cannot exclude the possibility of low-level epimerization. Thus, in practice it is probably safest to focus on cyclization sites such as Gly-Xaa or Pro-Xaa (Xaa denotes any amino acid), and these residues are abundantly found in cyclic disulfide-rich peptides.[38]

Cyclization of the partially protected and relatively long peptides proceeded cleanly and rapidly in all cases studied, resulting in high yields (~10%, based on quantity set up to be cyclized) of isolated cyclic, reduced peptide. At a peptide concentration of 2 mM, we were unable to detect any formation of dimers or higher order oligomers by high-resolution LC-MS. Table 1 shows a comparison of isolated product yields for KB1 and MCoTI-II obtained via the established Boc-SPPS/NCL strategy utilizing unprotected peptides[11] and the new Fmoc approach utilizing partially protected peptide segments in the cyclization step. In the case of KB1, yields are comparable between both approaches, whereas MCoTI-II was obtained in better yields via the Boc-SPPS/NCL strategy. This discrepancy is likely caused by less efficient peptide chain assembly during Fmoc-SPPS. The products were folded, and disulfides formed through random oxidation of cysteines, which in nearly all cases yielded the correctly disulfide-bonded isomer as judged by detailed HPLC and ^{1}H NMR spectroscopic analysis. In some cases additional isomers were observed, and in the cases of parigidin-br-1 or [L6-RGDS]kalata B1 only misfolded material (incorrectly disulfide bonded isomers) could be recovered. In the case of [L6-RGDS]kalata B1 this behavior is likely caused by drastic shortening of the β-hairpin region of loop 6 as a result of replacing the native heptapeptide sequence TRNGLPV with the tetrapeptide RGDS. In general, observing more than one set of disulfide-bond pairings during oxidation is not surprising, as peptides containing six cysteine residues can potentially give rise to up to 15 different disulfide bonded isomers. This multiplicity can be overcome by strategic placement of orthogonally protected cysteine pairs and directed or semi-directed disulfide formation strategies. However, there is generally little need to use orthogonal protecting strategies for the production of Möbius and trypsin inhibitor cyclotides because the major isomer normally contains the desired native connectivity. As the majority of the peptides assembled for this study belong to these two classes, orthogonal Cys-protecting groups were not explored. We expect that the Fmoc cyclization method described here will be more versatile than the established Boc-NCL procedure, because this new approach does not rely on an N-terminal cysteine and because of the greater variety and better compatibility of orthogonally side-chain-protected Fmoc-Cys building blocks.[39] The new Fmoc approach avoids the use of highly toxic HF and thus is also compatible with a range of HF-sensitive abiotic functionalities that can be useful for studying these molecules in vitro and in vivo (e.g., fluorophores, azides for "click chemistry", or diazirine-based photoaffinity labels). Removing the need for HF adds value to this methodology in the preclinical research arena as well as in generating drug substances for clinical studies.

In summary, we have described a rapid, mild, and cost efficient alternative method for synthesizing complex disulfide-rich cyclic peptides via automated Fmoc chemistry. Because of its simplicity and broad applicability, we expect this approach will prove to be an important advantage in the growing field of disulfide-rich cyclic peptides.

EXPERIMENTAL SECTION

Liquid Chromatography (LC) and Mass Spectrometry (MS). Peptides were purified on an ultrafast liquid chromatography (UFLC) system equipped with a UV−vis detector recording at 214 and 280 nm and a C18 250 × 21 mm, 5 μm column. Solvent A: 0.05% TFA in H_2O; solvent B: 0.045% TFA, 10% H_2O, 90% acetonitrile (ACN). Electrospray ionization mass spectrometry (ESI-MS) and LC-MS were carried out on an UFLC system with a detector set to monitor 214 and 280 nm wavelengths and a C18, 150 × 2 mm, 5 μm, column. Solvent A: 0.05% formic acid (FA) in H_2O; solvent B: 0.045% FA, 10% H_2O, 90% ACN.

Peptide Assembly. Peptides were synthesized by Fmoc SPPS on an automated peptide synthesizer using standard protocols. The following side-chain protecting groups were used: Cys(Trt), Asp(tBu), Glu(tBu), Lys(Boc), Asn(Trt), Arg(Pbf), Ser(tBu), Thr(tBu), Trp(Boc), and Tyr(tBu). The 2-CTC resin (substitution value 0.8 mmol/g, 0.125 mmol per reaction vessel, two reaction vessels per synthesized peptide) was swollen in DCM. The first amino acid was coupled onto the resin for 1 h in a 1:1 mix of DMF and DCM, with a 4-fold excess of amino acid and 8-fold excess of DIPEA followed by addition of 1.25 mL of methanol (MeOH) and further mixing for 15 min to cap any remaining reactive functionalities on the resin. The resin was washed with DMF, DCM, MeOH, and DMF. Fmoc deprotection was carried out with piperidine in DMF (1:2 (v/v)) twice for 3 min. Subsequent amino acids were coupled twice for 10 min using an amino acid/1*H*-benzotriazolium-1-[bis(dimethylamino)methylene]-5-chloro-hexafluorophosphate-(1-),3-oxide (HCTU)/DIPEA ratio of 4:4:8 relative to resin loading. DMF was used for resin washing between deprotection and coupling steps. After chain assembly was complete, the terminal Fmoc group was removed and the resin washed with DMF and DCM and dried under a flow of nitrogen for 2 h.

Cyclization and Removal of Side-Chain-Protecting Groups. To obtain the cyclic reduced peptide, a three-step procedure was followed (Scheme 1 and Supporting Information Scheme S1). The first step involved cleaving the peptide off the resin while leaving the side-chain protecting groups intact. The dried peptide resin (an average of 1.4 g was obtained per synthesis) was placed in a fritted reaction vessel and treated 10 times with 5 mL of 1% TFA in DCM (v/v) for 5 min. The eluates were collected and combined into a round-bottomed flask containing 150 mL of 50% ACN, 0.05% TFA in water (v/v). DCM and TFA were removed under vacuum, and the resulting solution was lyophilized. A 800 mg amount of the crude side-chain-protected peptide was dissolved in DMF at a concentration of 2 mM in a round-bottom flask. Solid *N*,*N*,*N*′,*N*′-tetramethyl-*O*-(7-

dx.doi.org/10.1021/jo500699m | J. Org. Chem. 2014, 79, 5538−5544

azabenzotriazol-1-yl)uronium hexafluorophosphate (HATU) was added to the solution to give a final concentration of 5 mM and mixed for 30 s. DIPEA was added to a final concentration of 10 mM, and the solution was stirred for 3 h at room temperature. The mixture was diluted with twice the volume of 50% ACN (0.05% TFA) and lyophilized overnight. Side-chain deprotection was carried out by adding 50 mL of triisopropylsilane (TIPS):H_2O:TFA (2:2:96, (v/v/v)) per 800 mg of crude peptide and stirring the mixture for 2.5 h at room temperature. The majority of the TFA was evaporated under vacuum, and the peptide precipitated with ice-cold diethyl ether. Peptide was dissolved in 50% ACN (0.05% TFA) and lyophilized.

Purification of the Cyclic Reduced Peptide. Cyclic reduced peptides were purified by reversed-phase HPLC (RP-HPLC). Briefly, the peptides were dissolved in 100 mL of 7% solvent B, filtered through a 0.45 μm syringe filter, and loaded onto the 21 mm column. After loading, the column was washed with the 7% solvent B for 30 min. Cyclic peptides were purified on the semipreparative system using a linear gradient from 7% to 70% solvent B over 70 min, at a flow rate of 8 mL/min. Fractions were collected over the course of the chromatography run and analyzed by ESI-MS. Fractions containing the desired product were pooled and lyophilized.

Disulfide Formation and Folding. Purified reduced cyclic peptides were oxidized and folded as previously described.[11,40] Briefly, oxidations of kalata B1 and variants thereof were carried out in a solution containing 50% 2-propanol, 0.1 M NH_4HCO_3, 2 mM reduced glutathione (pH 8.3). Cyclic MCoTI-II was dissolved at 0.1 mg/mL in a buffer containing 0.1 M NH_4HCO_3, 2 mM reduced glutathione (pH 8.3), and both oxidative solutions were stirred 48 h at room temperature. Parigidin-br-1 was set up to oxidize at 0.5 mg/mL in 10% DMSO, 10% ACN, 10% 2,2,2-trifluoroethanol (TFE), 1 M guanidine hydrochloride (GnCl), 0.1 M NH_4HCO_3 at pH 8.3. All folding reaction products were purified by semipreparative RP-HPLC as described above. Peptide purities were assessed on a LC-MS system with a gradient from 2% to 82% of solvent B in solvent A over 40 min at a flow rate of 0.3 mL/min (Table 1 and Supporting Information Figure S1).

Boc SPPS, NCL Cyclization, and Oxidative Folding. KB1 and MCoTI-II peptides were assembled using Boc SPPS, NCL cyclized, and oxidized as described by Daly et al.[11] However, 2 × 5 min couplings using HCTU as opposed to HBTU were used.

Nuclear Magnetic Resonance Spectroscopy. NMR measurements were carried out on a Bruker Avance 600 MHz NMR spectrometer equipped with a cryoprobe at 298 K. Peptide samples were prepared in 90% H_2O/10% D_2O at ∼1 mM and pH ∼4. Chemical shifts were referenced to sodium 2,2-dimethyl-2-silapentane-5-sulfonate (DSS). Spectra recorded were one-dimensional (1D) ^{1}H and two-dimensional (2D) total correlated spectroscopy (TOCSY)[41] (Supporting Information Figure S3) and NOESY[42] (200 ms mixing time) spectra. All 2D spectra were recorded in phase-sensitive mode using time-proportional incrementation for quadrature detection in the t_1 dimension.[43] Water suppression was achieved using excitation sculpting gradients.[44] Spectra were acquired with 4096 data points in the F_2 dimension and 512 data points in the F_1 dimension. The t_1 dimension was zero-filled to 1024 real data points. Spectra were processed using computer software and assigned in Xeasy[45] using the sequential assignment protocol.[46]

Circular Dichroism (CD) Spectroscopy. The secondary structure of native kalata B1, D-kalata B1 as well as a racemic mixture of the two enantiomers was evaluated by CD spectroscopy.[47] Peptide solutions were prepared in H_2O at a concentration of 25 μM and analyzed in quartz cuvettes with 0.1 cm path length. CD spectra were recorded on a spectropolarimeter using 50 nm/min scan speed over a range of 190−260 nm at room temperature. The CD signal averaged from five scans was normalized by subtracting the solvent contribution and converting to mean residue molar ellipticity $[\theta]_{MR}$.

■ ASSOCIATED CONTENT

Supporting Information

Fmoc vs Boc cyclization chemistry diagram (Scheme S1), analytical HPLC and mass spectra of crude cyclic and final oxidized compounds (Figures S1 and S2), and TOCSY NMR spectra of correctly folded peptides (Figure S3). This material is available free of charge via the Internet at http://pubs.acs.org.

■ AUTHOR INFORMATION

Corresponding Author

*Tel: +61 7 3346 2019. E-mail: d.craik@imb.uq.edu.au.

Author Contributions

§These authors contributed equally to this work

Notes

The authors declare no competing financial interest.

■ ACKNOWLEDGMENTS

This work was supported by an Australian Research Council Linkage grant (LP110200213), the Queensland Government Smart Future Co-investment Fund, and Pfizer Corporation. D.J.C. is a National Health and Medical Research Council Professorial Fellow (APP1026501). We thank Peta Harvey and Lai Yue Chan for NMR support.

■ REFERENCES

(1) Craik, D. J.; Daly, N. L.; Bond, T.; Waine, C. *J. Mol. Biol.* **1999**, *294*, 1327.

(2) Koehbach, J.; Attah, A. F.; Berger, A.; Hellinger, R.; Kutchan, T. M.; Carpenter, E. J.; Rolf, M.; Sonibare, M. A.; Moody, J. O.; Wong, G. K.; Dessein, S.; Greger, H.; Gruber, C. W. *Biopolymers* **2013**, *100*, 438.

(3) Göransson, U.; Burman, R.; Gunasekera, S.; Stromstedt, A. A.; Rosengren, K. J. *J. Biol. Chem.* **2012**, *287*, 27001.

(4) Colgrave, M. L.; Craik, D. J. *Biochemistry* **2004**, *43*, 5965.

(5) Ji, Y.; Majumder, S.; Millard, M.; Borra, R.; Bi, T.; Elnagar, A. Y.; Neamati, N.; Shekhtman, A.; Camarero, J. A. *J. Am. Chem. Soc.* **2013**, *135*, 11623.

(6) Chan, L. Y.; Gunasekera, S.; Henriques, S. T.; Worth, N. F.; Le, S. J.; Clark, R. J.; Campbell, J. H.; Craik, D. J.; Daly, N. L. *Blood* **2011**, *118*, 6709.

(7) Wang, C. K.; Gruber, C. W.; Cemazar, M.; Siatskas, C.; Tagore, P.; Payne, N.; Sun, G.; Wang, S.; Bernard, C. C.; Craik, D. J. *ACS Chem. Biol.* **2014**, *9*, 156.

(8) Poth, A. G.; Chan, L. Y.; Craik, D. J. *Biopolymers* **2013**, *100*, 480.

(9) Wong, C. T.; Rowlands, D. K.; Wong, C. H.; Lo, T. W.; Nguyen, G. K.; Li, H. Y.; Tam, J. P. *Angew. Chem., Int. Ed.* **2012**, *51*, 5620.

(10) White, C. J.; Yudin, A. K. *Nat. Chem.* **2011**, *3*, 509.

(11) Daly, N. L.; Love, S.; Alewood, P. F.; Craik, D. J. *Biochemistry* **1999**, *38*, 10606.

(12) Tam, J. P.; Lu, Y.-A.; Yu, Q. *J. Am. Chem. Soc.* **1999**, *121*, 4316.

(13) Tam, J. P.; Lu, Y. A.; Yang, J. L.; Chiu, K. W. *Proc. Natl. Acad. Sci. U.S.A.* **1999**, *96*, 8913.

(14) Dawson, P. E.; Muir, T. W.; Clark-Lewis, I.; Kent, S. B. *Science* **1994**, *266*, 776.

(15) Hackeng, T. M.; Griffin, J. H.; Dawson, P. E. *Proc. Natl. Acad. Sci. U.S.A.* **1999**, *96*, 10068.

(16) Mende, F.; Seitz, O. *Angew. Chem., Int. Ed.* **2011**, *50*, 1232.

(17) Carpino, L. A.; Han, G. Y. *J. Org. Chem.* **1972**, *37*, 3404.

(18) Saether, O.; Craik, D. J.; Campbell, I. D.; Sletten, K.; Juul, J.; Norman, D. G. *Biochemistry* **1995**, *34*, 4147.

(19) Pinto, M. F.; Fensterseifer, I. C.; Migliolo, L.; Sousa, D. A.; de Capdville, G.; Arboleda-Valencia, J. W.; Colgrave, M. L.; Craik, D. J.; Magalhaes, B. S.; Dias, S. C.; Franco, O. L. *J. Biol. Chem.* **2012**, *287*, 134.

(20) Hernandez, J. F.; Gagnon, J.; Chiche, L.; Nguyen, T. M.; Andrieu, J. P.; Heitz, A.; Trinh Hong, T.; Pham, T. T.; Le Nguyen, D. *Biochemistry* **2000**, *39*, 5722.

(21) Felizmenio-Quimio, M. E.; Daly, N. L.; Craik, D. J. *J. Biol. Chem.* **2001**, *276*, 22875.
(22) Rosengren, K. J.; Daly, N. L.; Plan, M. R.; Waine, C.; Craik, D. J. *J. Biol. Chem.* **2003**, *278*, 8606.
(23) Wishart, D. S.; Bigam, C. G.; Holm, A.; Hodges, R. S.; Sykes, B. D. *J. Biomol. NMR* **1995**, *5*, 67.
(24) Simonsen, S. M.; Sando, L.; Rosengren, K. J.; Wang, C. K.; Colgrave, M. L.; Daly, N. L.; Craik, D. J. *J. Biol. Chem.* **2008**, *283*, 9805.
(25) Heitz, A.; Hernandez, J. F.; Gagnon, J.; Hong, T. T.; Pham, T. T.; Nguyen, T. M.; Le-Nguyen, D.; Chiche, L. *Biochemistry* **2001**, *40*, 7973.
(26) Leta Aboye, T.; Clark, R. J.; Craik, D. J.; Goransson, U. *ChemBioChem* **2008**, *9*, 103.
(27) Gunasekera, S.; Daly, N.; Clark, R.; Craik, D. J. *Antioxid. Redox Signal.* **2009**, *11*, 971.
(28) Sando, L.; Henriques, S. T.; Foley, F.; Simonsen, S. M.; Daly, N. L.; Hall, K. N.; Gustafson, K. R.; Aguilar, M. I.; Craik, D. J. *ChemBioChem* **2011**, *12*, 2456.
(29) Merrifield, R. B. *J. Am. Chem. Soc.* **1963**, *85*, 2149.
(30) Gunasekera, S.; Aboye, T. L.; Madian, W. A.; El-Seedi, H. R.; Göransson, U. *Int. J. Pept. Res. Ther.* **2013**, *19*, 43.
(31) Taichi, M.; Hemu, X.; Qiu, Y.; Tam, J. P. *Org. Lett.* **2013**, *15*, 2620.
(32) Park, S.; Gunasekera, S.; Aboye, T. L.; Göransson, U. *Int. J. Pept. Res. Ther.* **2010**, *16*, 167.
(33) Blanco-Canosa, J. B.; Dawson, P. E. *Angew. Chem., Int. Ed.* **2008**, *47*, 6851.
(34) Zheng, J. S.; Chang, H. N.; Wang, F. L.; Liu, L. *J. Am. Chem. Soc.* **2011**, *133*, 11080.
(35) Zheng, J. S.; Tang, S.; Guo, Y.; Chang, H. N.; Liu, L. *ChemBioChem* **2012**, *13*, 542.
(36) Carpino, L. A.; Imazumi, H.; El-Faham, A.; Ferrer, F. J.; Zhang, C.; Lee, Y.; Foxman, B. M.; Henklein, P.; Hanay, C.; Mugge, C.; Wenschuh, H.; Klose, J.; Beyermann, M.; Bienert, M. *Angew. Chem., Int. Ed.* **2002**, *41*, 441.
(37) Carpino, L. A. *J. Am. Chem. Soc.* **1993**, *115*, 4397−4398.
(38) Wang, C. K.; Kaas, Q.; Chiche, L.; Craik, D. J. *Nucleic Acids Res.* **2008**, *36*, D206.
(39) Isidro-Llobet, A.; Alvarez, M.; Albericio, F. *Chem. Rev.* **2009**, *109*, 2455.
(40) Cěmažar, M.; Daly, N. L.; Haggblad, S.; Lo, K. P.; Yulyaningsih, E.; Craik, D. J. *J. Biol. Chem.* **2006**, *281*, 8224.
(41) Braunschweiler, L.; Ernst, R. R. *J. Magn. Reson.* **1983**, *53*, 521.
(42) Jeener, J.; Meier, B. H.; Bachmann, P.; Ernst, R. R. *J. Chem. Phys.* **1979**, *71*, 4546.
(43) Marion, D.; Wüthrich, K. *Biochem. Biophys. Res. Commun.* **1983**, *113*, 967.
(44) Hwang, T. L.; Shaka, A. J. *J. Magn. Reson.* **1995**, *112*, 275.
(45) Bartels, C.; Xia, T. H.; Billeter, M.; Guntert, P.; Wuthrich, K. *J. Biomol. NMR* **1995**, *6*, 1.
(46) Wüthrich, K. *NMR of Proteins and Nucleic Acids*; Wiley-Interscience: New York, 1986.
(47) Greenfield, N. J. *Nat. Protoc.* **2006**, *1*, 2876.